YEARLY PROGRESS REPORT

Project Title: Spray Rolling Aluminum Strip

Covering Period: April 1, 2001 through March 31, 2002

Date of Report: February 10, 2003

Recipient:
University of California, Irvine
160 Administration Building
Irvine, CA 92697

Award Number: DE-FC07-00ID13816

Subcontractors:
Jean-Pierre Delplanque
Colorado School of Mines
Engineering Division
Golden, CO 80401

Other Partners:
Kevin M. McHugh
Idaho National Engineering and Environmental Laboratory
Idaho Falls, ID 83415

Contact(s):
Enrique J. Lavernia
University of California, Irvine
Department of Chemical Engineering and Materials Science
Irvine, CA 92697-2575
Tel: (949) 824-8277, 8714; Email: lavernia@uci.edu

Project Team:
Simon Friedrich
Office of Industrial Technologies
U.S. Department of Energy
Washington D.C. 20585

John Yankeelov
Idaho Operations Office
U.S. Department of Energy
Idaho Falls, ID 83401

David Leon and Greg Hildeman
Alcoa Technical Center

Scott Goodrich
Pechiney Rolled Products

Viren Goyal
Inductotherm Corp.

Robert Hayes

Yearly Progress Report
DE-FC07-00ID13816
Metal Technology, Inc.

Project Objective:
The objective of this project is to demonstrate the feasibility of the spray rolling process at the bench-scale level and evaluate materials properties of spray rolled aluminum strip alloys, as shown in Figure 1. Also it will demonstrate 2X scalability of the process and document technical hurdles to further scale up and initiate technology transfer to industry for eventual commercialization of the process. Spray rolling combines spray forming, identified as a key need in the Aluminum Industry Technology Roadmap, with rolling for the net-shape manufacturing of aluminum strip.

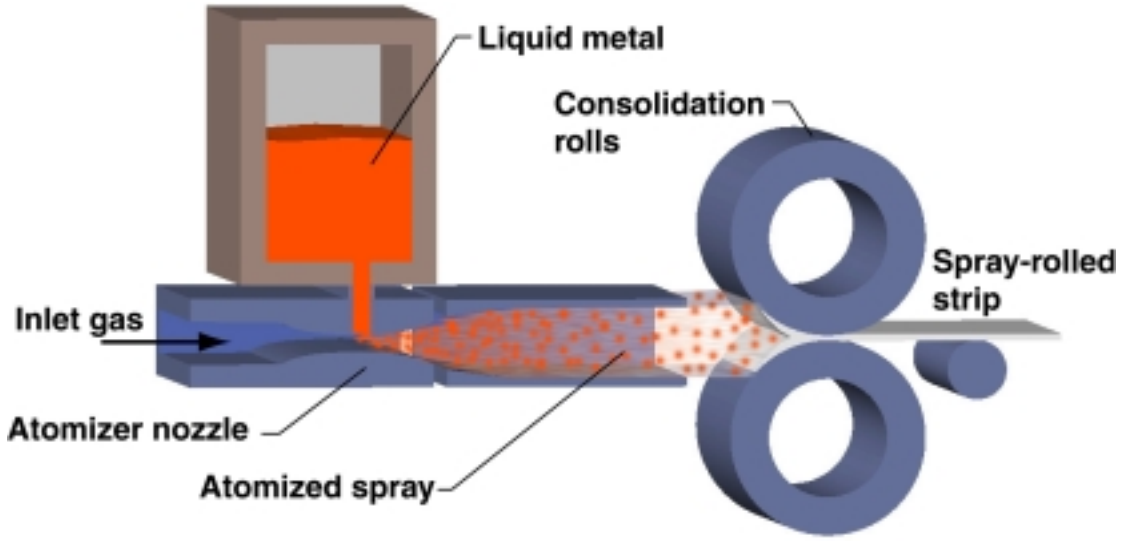

Figure 1 Schematic of the spray rolling process.

Background:
Spray forming is a competitive low-cost alternative to ingot metallurgy for manufacturing ferrous and non-ferrous alloy shapes. It produces materials with a reduced number of processing steps, while maintaining materials properties, with the possibility of near-net-shape manufacturing. However, there are several hurdles to large-scale commercial adoption of spray forming: 1) ensuring strip is consistently flat, 2) eliminating porosity, particularly at the deposit/substrate interface, and 3) improving material yield. Spray rolling is an innovative manufacturing technique to produce aluminum net-shape products. It combines benefits of twin-roll casting and conventional spray forming, showing a promising potential to overcome the above hurdles associated with spray forming. Spray rolling requires less energy and generates less scrap than conventional processes and, consequently, enables the development of materials with lower environmental impacts in both processing and final products.

In previous year the following work has been completed: (1) Definition of the facility modifications; (2) Procedure of the equipment and feedstock materials from industrial partners; (3) Definition of processing conditions for spray forming and reactive spray forming; (4) Preliminary spray forming experiments for correlation between microstructure and processing parameters; (5) Development of numerical method for investigation of spray behavior; (6) Assembling and testing of spray rolling equipment; and (7) Preliminary experiment of spray

rolling of aluminum alloys for evaluation of microstructure, materials properties, and influence of the processing parameters on strip quality.

Status:

During the reporting year, main research activities were focused on process optimization via understanding of fundamental phenomena, modeling development, and characterization of spray rolled materials. To review the project progress, Quarterly review meetings were held at UC Irvine on April 03, 2001, Inductotherm Corp. (Rancocas, NJ) on July 25, 2001, DOE Annual Review Meeting (Lexington, Kentucky) on October 18, 2001, and Pechiney Rolled Products (Ravenswood, WV) on January 31, 2002, respectively. During the reporting period, main research accomplishments are summarized below:

1. Understanding of Fundamental Phenomena

1.1 Reactive spray forming

Reactive spray forming experiments of 5083 Al were conducted. Purpose of the experiments was to optimize the processing parameters for formation and optimal volume fraction of oxide dispersoids, and their influences in microstructural evolution of the deposited materials. These include the effects of reactive atomization on the dynamic and thermal behavior of droplets during flight, the formation of oxides, microstructural evolution during deposition, the distribution, size and morphology of the oxides in the deposited and secondary-worked materials, and the mechanism of oxide fragmentation during deposition and during secondary working. The results showed that the droplet dynamics are altered by the formation of the oxide on the droplet's surface. The droplet dynamics and the latent heat from the oxidation reactions have effects on the solidification of the droplets (see Figure 2). Figure 2 shows the history of temperature and solid fraction of a 82μm droplet atomized using N_2 and $10O_2$-$90N_2$ (vol. pct), respectively. The results also indicated that the undercooling experienced is similar (approximately 19°C) for both reactive atomization and nitrogen atomization.

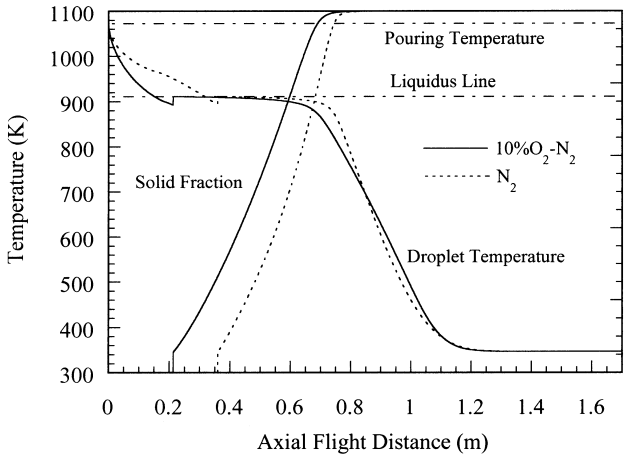

Figure 2 comparison of thermal behavior of 82μm

The deposited materials processed by RAD have a similar grain morphology to that of spray-formed materials. The sizes of oxide dispersoids in the deposited materials vary, from a few hundreds of nanometers to a few micrometers and are further fragmented into a few tens of nanometers through secondary working. On the basis of a uniaxial compressive assumption, the sizes of the fragmented oxide during deposition can be derived. Moreover, on the basis of the "maximum normal strain theory of failure", the final sizes of the oxide dispersoids can be estimated following secondary working processes (that will be discussed in the following sections).

1.2 Formation of oxide dispersoids

A droplet reacts with oxygen in the atomization gas mixture primarily during flight. Inspection of available numerical simulations on gas atomization of aluminum alloys indicates that it takes from a few to tens of milliseconds for a typical size droplet to attain low temperature (i.e., less than 300°C). As a result, a very thin oxide layer (less than a few hundred Angstroms) is expected, as confirmed by experiments [1-4]. As a consequence, an equation derived from the Mott-Cabrera theory of oxidation is used to estimate the oxidation rate:

$$\frac{\mathrm{d}X}{\mathrm{d}t} = A_0 \exp\left(-\frac{Q}{k_B T}\right) \cdot \exp\left(\frac{k_0 P^{1/2}}{k_B T X}\right) \qquad (1)$$

where X is the oxide thickness (Å), Q is the diffusion activation energy of metallic ions in the oxide (eV), P is the partial pressure of oxygen in the atomization gas mixture (torr), T is the droplet temperature (K) and k_B is the Boltzmann constant (eVK^{-1}). A_0 (Ås^{-1}) and k_0 (eVÅ torr$^{-1/2}$) are the constants related to the properties of the matrix and the metallic ions.

Fig. 3(a) shows the calculated oxide thickness on the surface of droplets from 10 to 300 μm in effective diameter. Oxide thickness increases with an increase of the effective diameter of the droplet; however, the thickness difference is not remarkable. As a consequence, the volume fraction of oxide increases rapidly with a decrease in effective diameter of the droplet, especially for small droplets, as shown in Fig. 3(a). Fig. 3(b) illustrates the evolution of oxide thickness on the droplet surface during flight. Independent of droplet size, the oxidation rate is extremely high and the oxide thickness increases sharply at the initial time period; subsequently, the oxidation rate becomes very slow and oxide thickness increases by a small amount. From the standpoint of the overall oxygen concentration in atomized powders with various sizes, the simulation results are in good agreement with experimental values obtained via chemical analysis.

Oxide fragmentation during deposition and secondary working process was investigated. Fig. 4(a) shows the diameters of the fragmented oxide discs as a function of effective diameter of droplets. The diameters of the oxide discs decrease with increasing effective droplet diameters. However, the diameters of the oxide discs are distributed from 0.5 to 3.6 μm for the droplets with an effective diameter from 10 to 300 μm, which is agreement with the SEM observations. According to the Zener pinning equation ($D_{\lim} = 4r/3f$), the effectiveness of oxide dispersoids with the size range from 0.5 to 3.6 μm to refine grain size is limited. Although there is intense deformation within the droplets when they impinge and flatten, the deformation may be concentrated on semi-solid droplets due to significant difference between the strength of the oxides and mushy droplets. Thus, secondary working is required to further fragment oxide dispersoids. Fig. 4(b) shows the calculated size of the oxide following extrusion plus rolling listed above. The oxide size is approximately 40 nm, regardless of the initial droplet size that is assumed. The calculated results are in good agreement with the TEM observations. Improvement of the oxide fragmentation model during secondary working processes, including rolling, extrusion and forging needs further effort.

Influences of processing parameters on oxygen concentration during reactive spray deposition were also investigated experimentally, with a particular attention on melt temperature and gas/melt flow ratio. Measurement of oxygen concentration via chemical analysis in both the

atomized 5083 Al powders and deposited material was conducted to determine the oxide volume fraction in the reactive spray deposited 5083 Al. Oxygen concentration in 5083 alloy was increased to 0.18 wt pct.

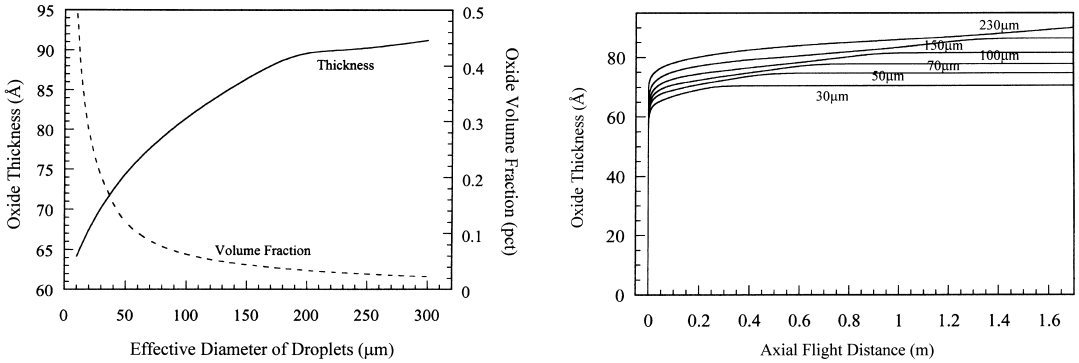

Figure 3 (a) Oxide thickness on the surface of droplets as a function of effective diameter (Left), and (b) Oxide thickness evolution during flight (Right).

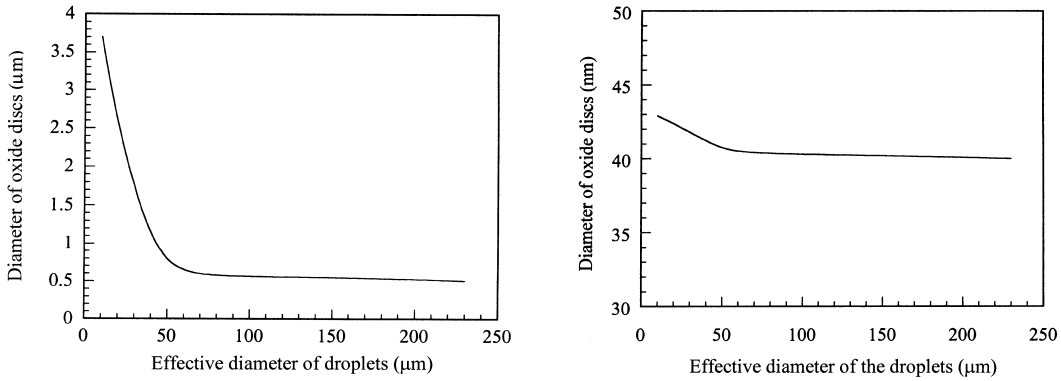

Figure 4 (a) The size of the oxide dispersoids in the deposited 5083 Al (Left), and (b) The size of the oxide dispersoids following rolling and extrusion (Right).

1.3 Microstructure analysis of reactive spray formed 5083 Al

Evolution of equiaxed grains from dendrite structure and grain growth mechanisms in the deposition stage was investigated to determine the role of the oxide dispersoids on grain refinement. Accordingly, distribution, constituent, phase of oxides in deposits were studied. Fig. 5 shows the results from microstructural characterization studies of the oxides in the deposited 5083 Al. Typically, the oxides are distributed in the following three types of spatial locations: grain boundaries, including triple points (Fig. 5(a)); grain interiors (Fig. 5(b)); and prior droplet boundaries, including the pore boundaries. The oxides assume plate-like morphology with size from 0.5-0.8μm. Upon impingement and flattening, the oxide film is fractured into dispersoids. Then, the temperature of the impinging droplets equilibrates. During equilibration, a small droplet absorbs thermal energy and is re-melted partially or completely; a large droplet loses heat and more solidification occurs within it. Following equilibration, the local phase state

(i.e., liquid or solid) on the boundary of two flattening droplets or the boundary between a flattening droplet and a pore, where there are oxide fragments, determines the distribution of the oxide dispersoids in the deposited materials. For example, with liquid phase on both sides of the boundary of two flattening droplets, the oxide fragments are pushed forward until the local liquid phase is exhausted and two or three grains meet together, leading to distribution of the oxide dispersoids at grain boundaries. With solid phases on both sides of the boundary of two

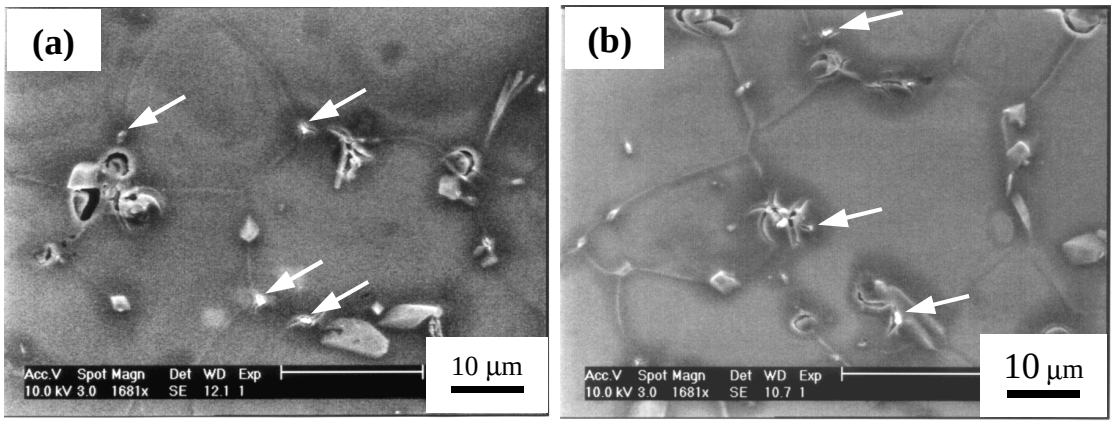

Figure 5 Distribution (SEM) of the oxides in the deposited 5083 Al: (a) grain boundaries and (b) grain interior.

flattening droplets, the oxide dispersoids remain along prior droplet boundaries.

Microstructure of the extruded 5083 Al (produced by reactive spray forming) was examined under as-extruded and following annealing at various temperatures. Figure 6 shows the TEM micrographs of the microstructure. Understanding of recrystallization kinetics of extruded 5083 Al was also explored, in order to determine appropriate rolling temperature to prevent recrystallization during spray rolling.

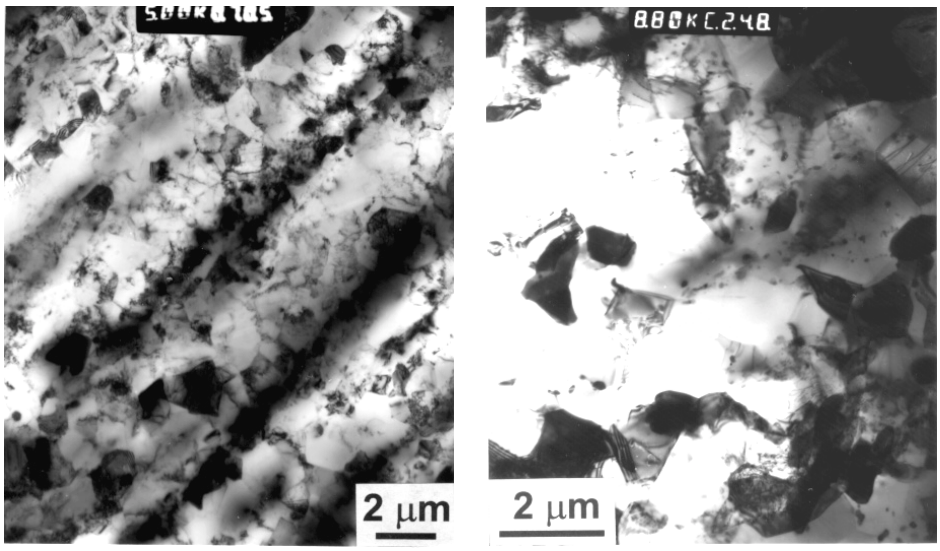

Figure 6 TEM microstructure of (a) As-extruded: deformed structure + recovered subgrains, average grain size ~0.7 μm; and (b) Extruded + annealed at 450 °C x 1h: recovered subgrains + recrystallized grains, average grain size ~1.5 μm (Right).

2. Modeling Development

2.1 Simulation and modeling of spray behavior in-flight

Computational fluid dynamics (CFD) tools were used to enhance the development and improvement of spray-based materials process, such as spray rolling. CFD simulations can be potentially used to evaluate the relative importance of various mechanisms (e.g., spray angle, droplet size and velocity distribution) on spray performance. In the preliminary study, flow field simulations in both conventional spray forming chamber and spray rolling chamber were conducted. Figure 7 shows the predicted thermal field as well as fluid particle paths characterizing the topology of the flow field induced in the spray rolling chamber, providing qualitative overview of the conditions in the chamber. More quantitative information, however, can be obtained from the two-dimensional projections.

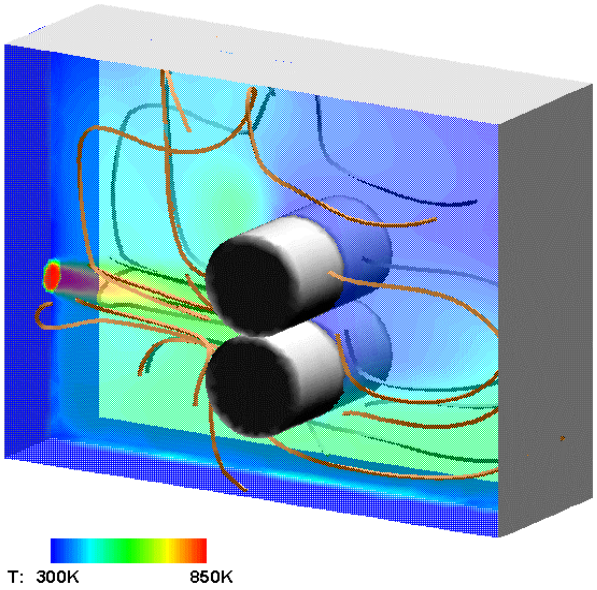

Figure 7 The 3D flow field in the spray rolling chamber evaluated using CFD.

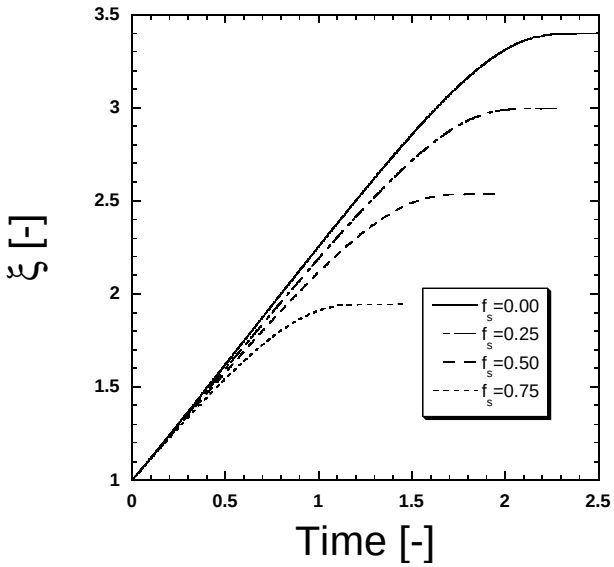

Figure 8 Solid fraction at impact has a significant effect on spreading dynamics.

2.2 Simulation and modeling of spray behavior at impact

A 2D numerical simulation tool based on RIPPLE (LANL) was improved to simulate droplet impact, spreading and solidification by solution of the Navier-Stokes and energy equation. These simulations help us determine if and how our reduced-order model for droplet impact should be modified to reflect INEEL's observation that incident droplets impinge on a "mushy layer". Figure 8 shows that solid fraction in metal droplets at impact has a significant effect on spreading dynamics of droplets. The reduced-order spreading and solidification model was also applied to enhance the oxide film breakup model. In addition, effort in improvement of droplet impact semi-analytical model was made to take into account the effect of non-ideal thermal contact at the droplet/substrate interface. 3D simulations of droplet impacts (without solidification) using TRUCHAS (LANL) were preliminarily conducted to provide validation tools for the semi-analytical model (low-order impact, spreading, and solidification).

2.3 Spray rolling model

A spray rolling model was developed to determine a suitable range for the spray deposition rate per unit length of the rolls. Figure 9 shows a geometric configuration of spray rolling process used for model set up. The key factors that may control the minimum spray deposition rate are identified to be either the removal of porosity or the removal of prior droplet boundaries. The mechanisms that control the maximum spray deposition rate are either the drag-in angle or the distance between the nozzle and deposited material's surface. Both the maximum and minimum spray deposition rates markedly increase with an increase of the roll diameter and rotational frequency of the rolls. Increasing rotational frequency of the rolls is an optimal approach to increase production rate of spray-rolled strips.

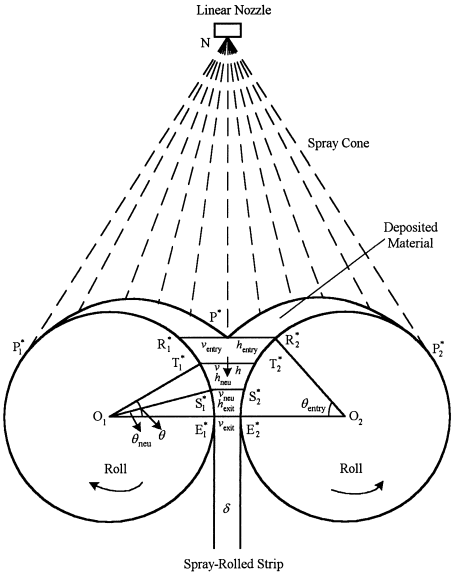

Figure 9 Schematic of spray rolling process.

3. Spray Rolling Facility and Materials Processing via Spray rolling

3.1 Spray rolling apparatus

Construction of the spray rolling apparatus was completed, as shown in Figure 10, with the following features: (1) Knife-edge strippers and strip guides were designed, constructed and installed to aid detachment of the aluminum strip from the rolls and proper feeding of the strip into the collection chamber. (2) Heated dams, used to define the width of the spray-rolled strip, were designed and constructed. Circuitry to monitor and control the temperature of the dams was designed and assembled. (3) A thermocouple to monitor the temperature of the rolls was installed. (4) A strip thickness gauge was installed. (5) Video equipment and CCD cameras were installed to monitor and record the aluminum spray impacting the rolls and the strip exiting the rolls.

Figure 10 Spray rolling facility: Front view (L) and side view (R).

3.2 Spray rolling of 3003 and 5083 Al alloys

The spray rolling unit was successfully used to produce preliminary strips in 4" and 8" wide of 3003 Al, and 5083 Al. Figure 11 shows the microstructures of 3003 Al produced using DC casting, twin-roll casting, spray deposition, and spray rolling. It can be seen that the photomicrograph of the spray rolled 3003 Al has demonstrated a more uniform microstructure (elimination of segregation, banding of constituent phases, poor grain morphology and porosity). It was found that liquid fraction of semisolid material and delivery to rolls are important factors in controlling strip microstructure and surface quality. 3003 Al was found to be much less sensitive to processing conditions (spray liquid fraction) than was 5083, primarily due to its narrower freezing range.

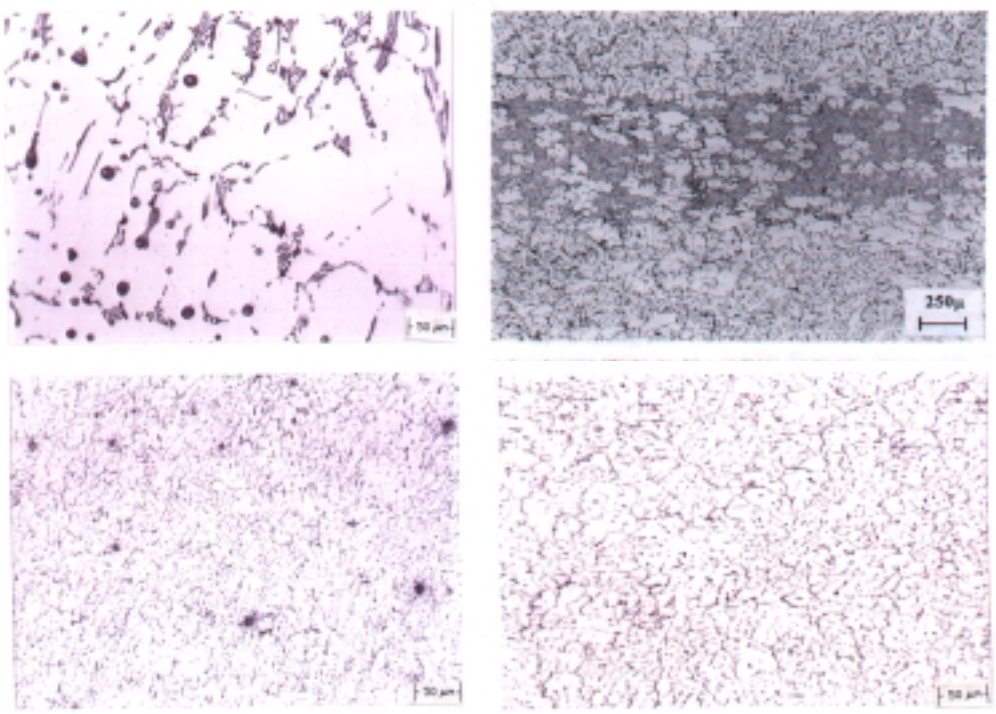

Figure 11 Photomicrographs of 3003 Al. DC Cast (upper left); Twin Roll Cast with Banding (upper right); Sprayed but not Rolled (lower left), Spray Rolled (lower right).

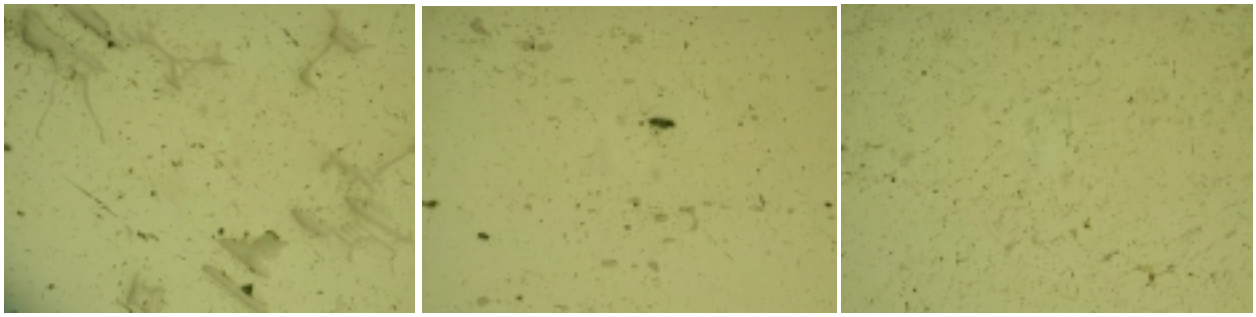

Figure 12 Photomicrographs of 5083 showing insoluble $(Fe,Mn)_3SiAl_{12}$ and $MnAl_6$ particles (gray). 500X, as polished. Cast (left); Commercial sheet (middle); Spray Rolled (right).

Microstructural analysis of as-spray-rolled 3003 Al and 5083 Al revealed a fine dispersion of $(Mn,Fe)_3SiAl_{12}$ and $(Mn,Fe)Al_6$ constituents, primarily near grain boundaries. Figure 12 shows the microstructure comparison between, cast, commercial sheet, and spray rolled strip of 5083 Al with a distribution of $(Mn,Fe)_3SiAl_{12}$ and $(Mn,Fe)Al_6$ constituents.

3.3 Post-thermal-mechanical processing of spray rolled Al

Spray-rolled 5083 and 3003 Al strips were thermomechanically processed. These recipes included stabilization annealing, recrystalization annealing, and cold working in various combinations, as shown in Figure 13. Annealing temperatures of 530^{O}C and 430^{O}C were used for 3003 Al, with soak times ranging from 10 minutes to 3 hrs. Cold reductions of up to 75% thickness reduction were performed. Annealing temperatures of 500^{O}C and 350^{O}C were used for 5083 Al, with soak times ranging from 10 minutes to 1 hr. Cold reductions of up to 50% thickness reduction were performed.

1. **As spray rolled (SR)**
2. **SR→ Ann (530^{O}C,10 min-3 hr.)→CR 35%**
3. **SR→ Ann (530^{O}C, 1 hr.) →CR 0%**
   ↓→CR 10%
   ↓→CR 20%
   ↓→CR 35%
   ↓→CR 55%
   ↓→CR 75%
4. **SR→ Ann (430^{O}C, 1 hr.) →CR 0%**
   ↓→CR 10%
   ↓→CR 20%
   ↓→CR 35%
   ↓→CR 55%
   ↓→CR 75%

1. **As-Spray Rolled**
2. **Spray Rolled→Stabilize Annealed (170^{O}C for 4 hrs.)**
   ↓→ Annealed (350^{O}C for 1 hr.)
   ↓→ Annealed (500 ^{O}C for 1 hr.)
3. **Spray Rolled→CR 50%→Stabilize Annealed (170^{O}C for 4 hrs.)**
   ↓→ Annealed (350^{O}C for 10 min.)
   ↓→ Annealed (500 ^{O}C for 10 min.)
4. **Spray Rolled→ Annealed (350 ^{O}C for 1 hr.) →CR 50%**
   ↓→ Annealed (500 ^{O}C for 1 hr.) →CR 50%
5. **SR→ Ann (350^{O}C,1 hr.)→CR 50%→ Ann (350^{O}C,10 min.)**
   ↓→ Ann (500 ^{O}C,1 hr.)→ ↑ ↓→ Ann (500 ^{O}C,10 min.)

Figure 13 Thermomechanically processing recipes for 3003 Al (Left) and 5083 Al (Right).

3.4 Mechanical testing of spray rolled Al alloys

Tensile properties (ultimate strength, yielding strength, and ductility) of spray-rolled 5083 and 3003 Al strips following thermomechanical processing were evaluated. The results showed that properties of the spray rolled Al strips exceeded (or at least comparable to, under some processing conditions) those of commercial sheet material. Tables 1 and 2 presents the tensile testing data of the spray rolled 5083 Al and 3003 Al under various conditions, respectively. Commercial data are also included for comparisons.

References:

1. G. Staniek: *Aluminum*, 60, 923 (1984).
2. G. Staniek, “Observation of Oxide Skin in Powder Metallurgy”, AFWAL-TR-83-4157, Air Force Wright Aeronautical Laboratories, Wright-Patterson Air Force Base, OH (1982).
3. W. S. Miller, I. R. Hughes, I. G. Palmer, N. P. Thomas, T. S. Saini and J. White, in *High Strength Powder Metallurgy Aluminum Alloys*, G. J. Hildeman and M. J. Koczak, eds., 311, the Met. Soc. AIME (1986).
4. J. W. Bohlen, R. J. Kar and G. R. Chaanani, in *Rapidly Solidified Aluminum Alloys*, 166, ASTM STP 890, M. E. Fine and E. A. Starke Jr., eds., ASTM Philadelphia (1986).

Table 1 Tensile data of the spray rolled 5083 Al under various conditions.

Condition	Ultimate Tensile Strength (ksi) typ (min)	Yield Strength (ksi) typ (min)	Elong. (%) typ (min)
Commercial O	42 (40)	21 (18)	22 (16)
Commercial H112	44 (40)	28 (18)	16 (12)
Commercial H116	46 (44)	33 (31)	16 (12)
Commercial H321	46 (44)	33 (31)	16 (12)
Commercial H323, H32	47 (45)	36 (34)	10 (8)
Commercial H343, H34	50 (50)	41 (39)	9 (6)
SR As-Deposited	31	26	6
SR-ANN 170^{O}C (4hr.)	38	25	13
SR-ANN 350^{O}C (1hr.)	32	25	6
SR-ANN 500^{O}C (1hr.)	41	21	20
SR-CR50%-ANN 170^{O}C (4 hr.)	51	44	4
SR-CR50%- ANN 350^{O}C (10 min.)	48	39	6
SR-CR50%-ANN 500^{O}C (10 min.)	43	23	17
SR-ANN 350^{O}C (1 hr.)-CR50%	52	49	2
SR-ANN 500^{O}C (1 hr.)-CR50%	59	53	4
SR- ANN 350^{O}C (1 hr.)-CR50%-ANN 350 ^{O}C (10 min)	44	34	3
SR- ANN 500^{O}C (1 hr.)-CR50%-ANN 500 ^{O}C (10 min)	44	23	25

Table 2 Tensile data of the spray rolled 3003 Al under various conditions.

Condition	Ultimate Tensile Strength (ksi) typ (min)	Yield Strength (ksi) typ (min)	Elong. at Failure (%) typ (min)
Commercial H14	22 (20)	21 (17)	8 (5)
SR (4” strip #1)-ANN (530^{O}C, 1 hr.)-CR35%	30	28	8
SR (4” strip #2)-ANN (430^{O}C, 1 hr.)-CR35%	30	29	8
SR (4” strip #2)-ANN (530^{O}C, 1 hr.)-CR35%	28	27	7
SR (4” strip #3)-ANN (530^{O}C, 1 hr.)-CR35%	27	26	9
SR (8” strip, center)-ANN (430^{O}C, 1 hr.)-CR35%	27	25	8
SR (8” strip, center)-ANN (530^{O}C, 1 hr.)-CR35%	26	25	9
SR (8” strip, edge)-ANN (430^{O}C, 1 hr.)-CR35%	29	27	9
SR (8” strip, edge)-ANN (530^{O}C, 1 hr.)-CR35%	26	25	8

Plan for Next Year:

Efforts in this year will emphasize demonstration of 2X scalability of the process and technology transfer. Specific issues to be explored are summarized as follows.

1.1 Explore issues related to process technology

- Evaluation of structure-properties of 5083 Al
- Database development for optimal process control of spray rolling including spray forming (SF) and reactive spray forming (RSF)
- Identify controlling mechanisms, improve grain size refinement mechanism and characterize microstructural evolution for RSF
- Finalize modeling of dispersoid distribution and volume fraction in RSF
- Continuously improve integrated process model to reflect experimental data and observations as they become available
- Database development for optimal process control using numerical simulation
- Identify controlling mechanisms
- Investigate numerically influence of dams on flow field within spray chamber and spray characteristics at impact on rolls.
- Scale atomizer for 8" wide strip
- Optimize process for wide melting range alloys such as 5083 and 6009.
- Evaluate superplasticity of 5083 and modified 5083.
- Install dams to contain transverse flow of metal to produce sharper edges on strip.

1.2 Explore issues related to technology transfer

- Establish technical feasibility of spray rolled 5083 Al for industrial applications such as automotive
- Characterization of steady-state operation conditions for scalability evaluation
- Simulation of steady-state operation conditions for scalability evaluation

1. 3 Explore Issues related to process economics

- Materials yield and cost
- Production rate
- Perform simulations as needed to explore the effect of various process parameters on yield and production rate

Patents: None.

Publications/Presentations:

Quarterly review presentations to industry participants, held at UC Irvine on April 03, 2001, Inductotherm Corp. (Rancocas, NJ) on July 25, 2001, and Pechiney Rolled Products (Ravenswood, WV) on January 31, 2002, respectively.

S.B. Johnson and J.-P. Delplanque: "A model for droplet spreading and solidification including impact angle, contact resistance, and undercooling effects," *Journal of Heat Transfer*, submitted for publication, 2002.

Y. J. Lin, Y. Zhou, and E. J. Lavernia: Presentation entitled “Spray Formed Al MMCs via In-Situ Reactions”, in *2001 TMS Fall Meeting on Affordable Metal-Matrix Composites for High Performance Applications*, Indianapolis, Indiana, Nov. 4-8, 2001.

Y. J. Lin, Y. Zhou, and E. J. Lavernia: in *Powder Materials: Current Research & Industrial Practices*, eds. F. D. Marquis, S. Thadhani, and N. Barrera, the Proceedings of a symposium in 2001 TMS Fall Meeting, The Minerals, Metals and Materials Society, Warrendale, PA, 2001, pp. 41-57.

Y. J. Lin, Y. Zhou, and E. J. Lavernia: “Microstructural Characterization of Oxides in 5083 Al Produced by Reactive Atomization and Deposition”, completed.

Y. J. Lin, Y. Zhou, and E. J. Lavernia: “On the Influences of in-Situ Reactions on Microstructure during Reactive Atomization and Deposition”, completed.

Yearly Progress Report
DE-FC07-00ID13816
Milestone Status Table:

ID No.	Description	Planned Completion Date	Actual Completion Date	Comments As of (03/31/02)
Task 1	**Spray Forming**	02/03		
1.1	Development of a semi-analytical model for droplet impact at an off-normal angle	12/2000	12/00	Completed
1.2	Characterization of sprayed 3003 and 5083 Al	01/2001	01/01	Completed
1.3	Perform numerical simulation of 3D droplet impact	06/2001	06/01	Completed
1.4	Adaptation of droplet in-flight model to spray forming/rolling configuration	12/2001	12/01	Completed
1.5	Correlate operating parameters with spray performance and resultant microstructure	10/2002		On Schedule
1.6	Database development for process control of spray rolling	02/2003		On Schedule
Task 2	**Reactive Spray Forming**			
2.1	Determine optimal operating parameters	03/2001	03/01	Completed
2.2	Develop a model of reactive spray forming for the prediction of dispersoid distribution and volume fraction	06/2002		On schedule
2.3	Comparison of predicted dispersoid distribution and volume fraction to experimental observation	11/2002		On Schedule
2.4	Conduct parametric studies to establish working relationships between process parameters and spray formed materials, and identify controlling mechanism	02/2003		On Schedule
2.5	Database development for reactive spray forming, and optimal process control for spray forming	02/2003		On Schedule
Task 3	**Spray Rolling**			
3.1	Design/construct spray rolling equipment and test by producing preliminary strip.	12/2000	12/00	Completed
3.2	Characterize preliminary strip and correlate with measured spray properties.	05/2001	05/01	Completed
3.3	Optimize/analyze spray rolled strip	02/2002		On Schedule
3.4	Scale by 2X and optimize strip and spray properties.	11/2002		On Schedule
Task 4	**Technology Development**			
4.1	Complete study of 3003 and 5083 Al alloys	02/2001	02/01	Completed
4.2	Establish technical feasibility of spray rolled 3003 Al strip for packaging and other application	02/2003		On Schedule
4.3	Establish technical feasibility of spray rolled 5083 Al strip for automobile	02/2003		On Schedule
Task 5	**Transition**			
5.1	Transfer equipment designs to industry, train industry personnel	02/2003		On Schedule
Task 6	**Management, Reporting, and Meetings**			
6.1	Quarterly report and review meeting			On schedule

Yearly Progress Report
DE-FC07-00ID13816
Budget Data:

			Approved Spending Plan			Actual Spent to Date		
Phase / Budget Period			DOE Amount	Cost Share	Total	DOE Amount	Cost Share	Total
	From	To						
Year 1	02/14/00	02/13/01	$112.3K	$229.8K	$342.2K	$117.2K	$229.8K	$346.9K
Year 2	02/14/01	02/13/02	107.7K	91.2K	197.9K	120.6K	91.2K	211.9K
Year 3								
Year 4								
Year 5								
Totals			220.0K	321.0K	540.1K	237.8K	321.0K	558.8K